Journal of Applied Mechanics and Technical Physics, Vol. 49, No. 6, pp. 985–991, 2008

SIMULATION OF MICELLAR–POLYMER FLOODING OF A LAYERED OIL RESERVOIR OF NONUNIFORM THICKNESS

N. S. Khabeev[1] **and N. A. Inogamov**[2]

UDC 532.546

The dynamics of oil displacement from a layered reservoir of nonuniform thickness consisting of two hydrodynamically connected layers of different absolute permeability is studied. Results of numerical calculations are given. The influence of the main determining factors on the oil displacement dynamics is studied.

Key words: *micellar–polymer flooding, filtration, nonuniform layered reservoir, numerical simulation.*

A promising method for increasing the reservoir production is micellar–polymer flooding [1]. Because of the low surface tension on the boundary of the micellar solution with the reservoir fluids, almost the entire oil is set in motion. The higher viscosities of the micellar solution and the injected spacer fluid bank (aqueous polymer solution) compared to the oil viscosity allow an increase in the displacement area.

As is known, real oil reservoirs are nonuniform, one of the main types of nonuniformity of porous media is permeability variation across a section of monolithic reservoirs [1]. We consider the profile problem [2] in a two-dimensional region. A mathematical model for micellar–polymer flooding is given in [3]. In [4], this model is extended to the case of nonuniform layered reservoirs, and in [5], to the case of pattern flooding in a well system.

The present paper gives the results of a numerical study of micellar–polymer flooding based on models [3–5] for the case of a nonuniform layered reservoir.

1. Oil Displacement from a Nonuniform Layered Reservoir with Specified Volume Flow Rate of the Injected Fluid. We consider various flooding modes in increasing order of complexity.

We first study oil displacement by water in an oil reservoir of nonuniform thickness consisting of two layers of different absolute permeability (Fig. 1). We solve the problem with a specified volume flow rate of the injected fluid $Q(t)$. Let the filtration region be a square ($l_y = l_x$). The parameters of the porous medium and the hydrodynamic parameters of the fluids (oil and water) being filtered are chosen as follows: $(s_\alpha^0)^* = 0$, $k_\alpha = (s_\alpha^0)^2$, $\mu_\alpha = \text{const}$, and $s_{10}^0 = 1$. We also set $Q(t) = 1$, $l_x = l_y = 1$, and $k^{(1)} = 1$. Figure 2 shows oil saturation isolines at the moment of injection of a water volume $0.2V_{\text{pore}}$, for uniform reservoir ($k^{(2)} = k^{(1)} = 1$) and nonuniform reservoir ($k^{(2)} = 6$).

Unlike in the uniform reservoir, the displacement dynamics in the reservoir of nonuniform thickness has the following features: in the high-permeability layer, the fluids move more rapidly, and although in the bottom low-permeability layer, the absolute permeability is the same as in the uniform layer, the fluids in it move more slowly. According to the problem formulation, the amount of the fluid injected into each layer is identical in the uniform and nonuniform cases. Therefore, the lower rate of displacement in the lower layer compared to that in the uniform layer is explained by the cross-flow of part of the fluid from this layer to the top layer. Hence, in the high-permeability layer, the filtration flux is higher. Nevertheless, with time, the displacement covers the entire zone of low permeability. In this case, according to the results of numerical calculations, the velocity of displacement in the bottom lower-permeability layer decreases. For example, let us determine the velocity of motion of the point at which only oil is present ($s^0 = 1$) at $y = 0$. This point is taken to be the position of the conditional displacement

[1]University of Bahrain, Manama 32038, Bahrain. [2]Lomonosov Moscow State University, Moscow 117234; nail@sci.uob.bh. Translated from Prikladnaya Mekhanika i Tekhnicheskaya Fizika, Vol. 49, No. 6, pp. 115–123, November–December, 2008. Original article submitted September 24, 2007.

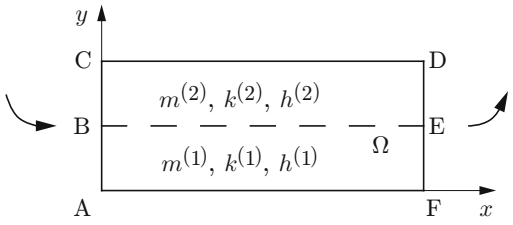

Fig. 1

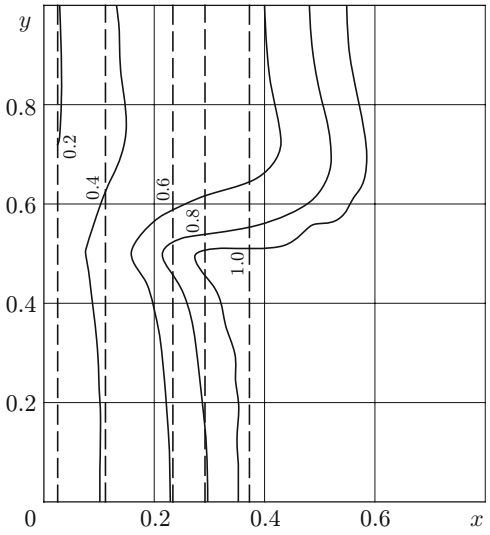

Fig. 2

Fig. 1. Nonuniform layered reservoir consisting of two layers.

Fig. 2. Oil saturation isolines for oil displacement by water from the uniform reservoir ($k^{(2)} = k^{(1)} = 1$) and nonuniform reservoir ($k^{(2)} = 6$ and $k^{(1)} = 1$) at $Q = 1$ ($p(1, y, t) = 1$), $s^0_{10} = 1$, $(s^0_{1\mathrm{w}})^* = (s^0_2)^* = 0$, $\mu_{\mathrm{oil}} = 1.8$, $\mu_{\mathrm{w}} = 1$, and $t = 0.2$: solid curves refer to the nonuniform reservoir; dashed curves to the uniform reservoir.

front. The horizontal coordinate x_{f} of this point changes with time, as follows: $x_{\mathrm{f}} = 0.35$ at $t = 0.2$, $x_{\mathrm{f}} = 0.57$ at $t = 0.5$, and $x_{\mathrm{f}} = 0.81$ at $t = 1$. This slow motion occurs because with time the oil saturation distribution in the vertical section of the reservoir becomes more and more nonuniform: in the highly porous layer, it is lower, and the relative amount of water in the top layer increases, and, hence, the displacement of the water-oil mixture in it is more rapid. Therefore, the amount of the injected fluid moving to the high-permeability layer increases with time. This effect, which depends monotonically on time, enhances in the period from the displacing-water breakthrough into the top layer to its breakthrough into the bottom layer.

The phase saturation isolines have a bend on the boundary separating the zones with different absolute permeability. From Fig. 2, it follows that the neighborhood of this boundary is the region which is the least covered by the displacement. This is because in the low-permeability layer of the indicated region, the fluid not only moves forward, as in the case of the uniform porous medium, but also flows into the high-permeability top layer. As a result, the velocity of motion of this part of the flow to the productive well decreases, and the fluid particles in it have longer trajectories. The indicated shape of the isoline located in the region of the high-permeability layer between the displacement fronts is also explained by the cross-flow from the bottom into this region. The cross-flow arises because of the lower pressure in this region of the high-permeability layer due to the filtration of the less viscous mixture in it. It is important to note that only oil cross-flow occurs since only oil is present in this zone of the low-permeability layer. The extent of this region increases to the moment of breakthrough.

An analysis of the calculated dependences of the relative amount of the extracted oil (the main parameter of oil production) on time $\eta(t)$ for a square filtration region for various values of the absolute permeability $k^{(2)}$ ($k^{(1)} = 1$) shows that since the layer originally contained only oil, oil recovery occurs immediately. The function η is linear up to the moment of breakthrough. At $t > t_{\mathrm{influx}}$, the value of η is larger the smaller the difference between the value of $k^{(2)}$ and the value of $k^{(1)} = 1$. In this case, the dependence of η on k is nonlinear. The difference in the oil recovery between the nonuniform and uniform reservoirs first increases but then decreases (after the water breakthrough into the low-permeability layer). In the case $k^{(2)} = 2$ at $t = 2$, the maximum oil production was 78% of the initial reserves. This is explained to some extent by the assumption of the model that the nature of the displacement does not depend on the filtration flow velocity. From the analysis performed, it can be argued that the displacement is similar in nature to the displacement in the case of isolated layers with one-dimensional filtration for various values of the volume flow rate of the injected water.

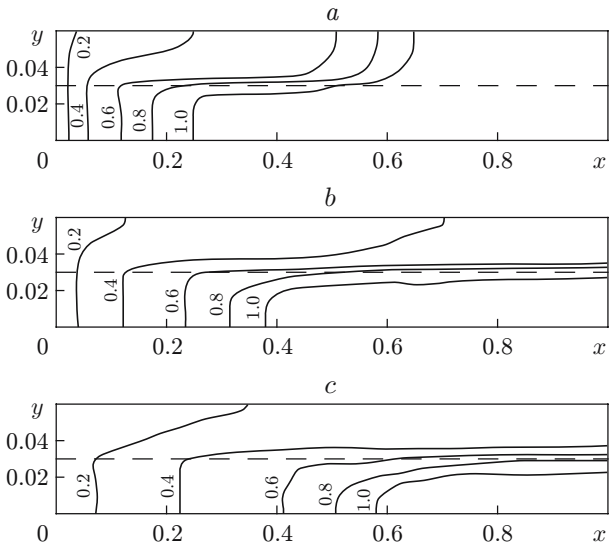

Fig. 3. Oil saturation isolines in a rectangular nonuniform reservoir at a specified flow rate ($Q = 1$) of the displacing water at the entrance and for $k^{(2)} = 4$ for $t = 0.2$ (a), 0.5 (b), and 1.0 (c).

The next flooding regime studied is oil displacement by water from a rectangular region, which is more consistent to the real structure of oil reservoirs (the initial and boundary conditions of the problem and the closing relations were the same as in the case considered above). The rectangle had the following dimensions: $l_x = 1$ and $h = 0.06$. Figure 3 shows the displacement dynamics for $k^{(2)} = 4$ at various times. (In Figs. 3–8, the dashed curve is the boundary separating the regions with different permeability.) The motion of the mixture in the low-permeability layer is nearly one-dimensional before the beginning of water discharge from the high-permeability layer.

A comparison of the results of the numerical simulation of flooding for various values of $k^{(2)}$ with the filtration calculations for the square region shows that, in layers of different permeability, the maximum relative distance between the rear boundaries of the regions in which the pore space is filled only with oil depends greatly not only on the degree of permeability nonuniformity but also on the reservoir shape. For example, for the square region for $k^{(2)} = 8$ and $t = 0.2$, this distance is 0.2, whereas for the rectangular region ($h = 0.06$), it is equal to 0.51. In addition, for a square regions with $k^{(2)} = 8$ and $k^{(2)} = 6$, this distance changes only slightly, whereas for the case of flooding of the examined rectangular region, its change is more insignificant. From an analysis of the numerical solutions, it also follows that, for the rectangular region, the time of water exit from the high-permeability layer depends on the degree of nonuniformity more significantly than for the case of the square region, for which this time remains almost unchanged in the range of $k^{(2)}$ considered. For the rectangular region, the current oil recovery coefficient was determined for constant absolute permeability of its top layer. For $k^{(2)} = 2$ and $t = 2$, the maximum oil recovery was 79% of the initial reserves (as in the case of the square reservoir), whereas for other, larger values of $k^{(2)}$, it is much lower. For example, for $k^{(2)} = 8$, $\eta(2) = 0.75$ for the square region and $\eta(0.2) = 0.64$ for the rectangular region. However, apparently, for larger time values, the effects of the degree of nonuniformity and the oil reservoir shape decrease.

Below, we consider the micellar–polymer flooding of a nonuniform-thickness oil reservoir consisting of two hydrodynamically connected layers of different absolute permeability. The geometrical shape of the layers corresponded to the structure of the reservoir for the last of the oil displacement regimes considered ($l_x = 1$ and $h = 0.06$). The problem was solved for a specified volume flow rate of the injected fluid. Since the thicknesses of the layers and their porosities were considered identical, it was assumed that the injection conditions in both layers are identical. The numerical calculations were performed for the following values of the hydrodynamic parameters of the reservoir system: residual phase saturations $(s_1^0)^* = 0.35$ and $(s_2^0)^* = 0.173$ and viscosities of the reservoir oil and water $\mu_{\text{oil}} = 4$ and $\mu_{\text{w}} = 1$. The curves of the relative phase permeabilities are the same as in [3–5]. Adsorption of surface-active substances (SASs) from the micellar solution by the porous skeleton was ignored, and absorption

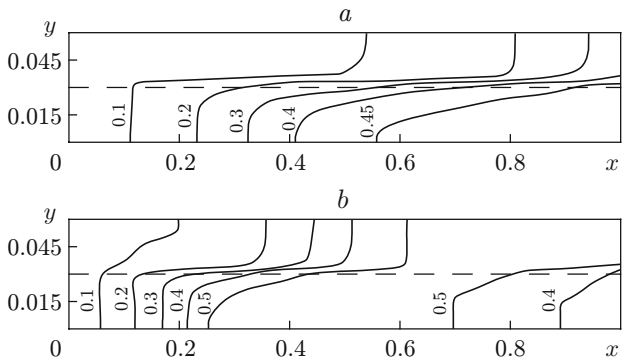

Fig. 4

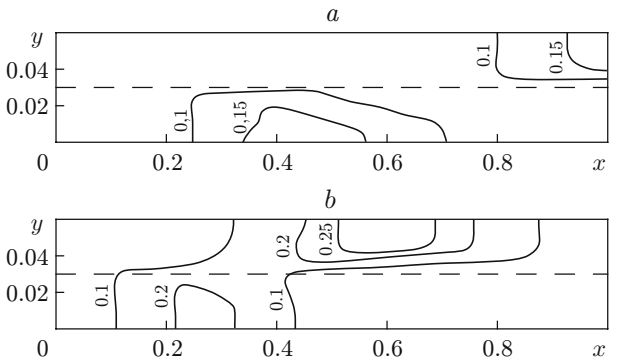

Fig. 5

Fig. 4. Isolines of the hydrocarbon saturation s_1^0 in a nonuniform rectangular layer ($k^{(2)} = 4$ and $k^{(1)} = 1$) for a specified flow rate ($Q = 1$) at the entrance in the case of micellar–polymer flooding ($t_\text{m} = 0.1$) for $t = 0.4$ (a) and 0.8 (b).

Fig. 5. Isolines of SAS concentration in the hydrocarbon phase $s_1^0 c_{1,3}$ ($t_\text{m} = 0.1$) for $t = 0.4$ (a) and 0.8 (b).

of the polymer was considered to obey Henry's law [6] with $\Gamma = 0.3$. The flooding regime considered was a tertiary oil recovery process: the initial oil concentration in the porous medium was equal to the residual oil saturation during flooding: $s_{10}^0 = (s_{1\text{w}}^0)^*$.

The results of the numerical simulation of the micellar–polymer displacement of residual oil in the system of layers are analyzed in the following sequence: 1) oil saturation distribution in the layer and the position of the main working agent — bank — versus the duration of the process for fixed values of the volume of the banks and the nonuniformity of the layers; 2) effect of the absolute permeability of the top layer $k^{(2)}$ on the effectiveness of displacement for the constant value $k^{(1)} = 1$.

Figures 4–7 correspond to the following parameters of micellar–polymer flooding: $s_{10}^0 = (s_{1\text{w}}^0)^* = 0.35$, $(s_2^0)^* = 0.173$, $\mu_\text{oil} = 4$, $\mu_\text{w} = 1$, $\mu_\text{m} = 21$, $\mu_\text{p} = 28$, and $t_\text{p} = 0.5$.

Figure 4 shows hydrocarbon saturation isolines at the times $t = 0.4$ and 0.8 for a layer with $k^{(2)} = 4$ for a bank volume $t_\text{m} = 0.1$. In Fig. 4a, it is evident that a water-oil bank is formed. As in the cases of oil displacement by water considered above, one-dimensional flow is observed in each layer with different volume flow rates. Figure 5 shows the position of the micellar fluid bank determined by SAS $s_1^0 c_{1,3}$ concentration isolines. It is evident that the part of the volume of the bank moving in the top high-permeability layer is greater and the SAS concentration in it is higher than in the lower layer. With time, the difference in the locations of the parts of the bank in the layers increases. The dimension of the zone occupied by them also increases, and the dimension of the region occupied by the highly concentrated solution decreases. The last two features of the micellar–polymer flooding regime also occur for one-dimensional motion.

Figure 6 shows isolines of the hydrocarbon fluid saturation and SAS concentration for a micellar bank volume $t_\text{m} = 0.02$. A comparison of the positions of the isolines of the micellar fluid bank and hydrocarbon fluid saturation for these two versions of residual oil displacement by various volumes of the micellar fluid (see Fig. 4–6) shows that the amount of the displaced oil initially contained in the reservoir is different in the cases considered. In both the high-permeability and low-permeability layers, the amount of the displaced oil is larger in the case of the flooding regime with a large volume of the micellar fluid bank.

Figure 7 shows isolines of the hydrocarbon saturation and SAS concentration in a nonuniform reservoir ($k^{(2)} = 10$) for a bank volume $t_\text{m} = 0.1$ at $t = 0.4$. In comparison to the case $k^{(2)} = 4$, the difference in the locations of the parts of the bank in the layers increased. In the case considered [$k^{(2)} = 10$], the positions occupied by the parts of the micellar fluid bank in the layers of different absolute permeability change differently with respect to their positions in Fig. 4 ($k^{(2)} = 4$): in the higher-permeability layer at the time studied $t = 0.4$, the bank advanced a smaller distance than the distance it is retarded in the bottom layer. In addition, the top layer at $k^{(2)} = 10$ contains a more concentrated solution than at $k^{(2)} = 4$, and in the bottom layer, its is less concentrated. Thus, for the isolines given in Fig. 7b and Fig. 6b, the maximum SAS concentration was 0.25. However, in the low-permeability layer, the dimension of the zone occupied by a solution with concentration not lower than the indicated value is

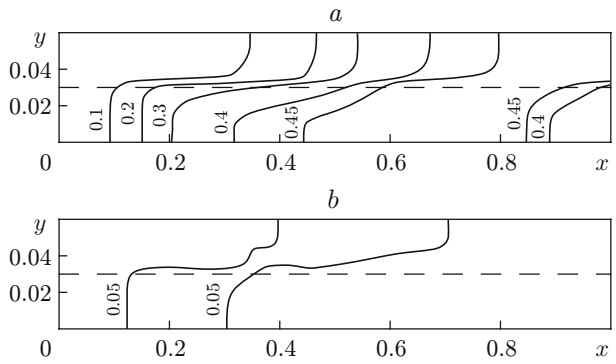

Fig. 6

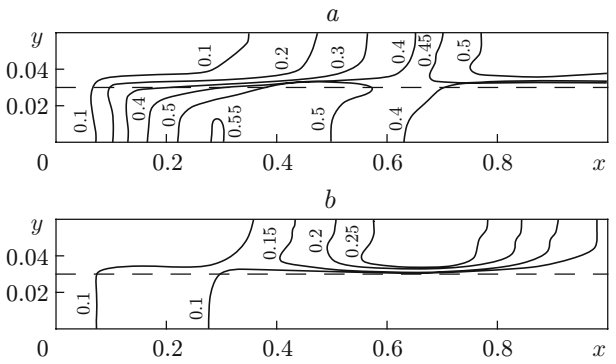

Fig. 7

Fig. 6. Isolines of hydrocarbon saturation s_1^0 (a) and SAS concentration $s_1^0 c_{1,3}$ (b) in the case of micellar–polymer flooding ($t_{\text{m}} = 0.02$) of a nonuniform reservoir ($k^{(2)} = 4$ and $k^{(1)} = 1$) at $t = 0.4$.

Fig. 7. Isolines of hydrocarbon saturation (a) and SAS concentration (b) in the case of micellar–polymer flooding ($t_{\text{m}} = 0.1$) of a nonuniform reservoir ($k^{(2)} = 10$ and $k^{(1)} = 1$) at $t = 0.4$.

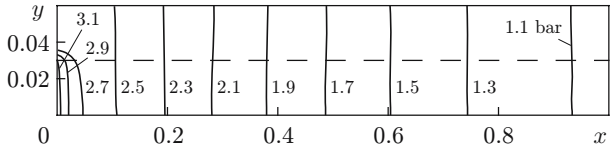

Fig. 8. Isobars in the case of micellar–polymer flooding ($t_{\text{m}} = 0.1$) of a nonuniform rectangular reservoir ($k^{(2)} = 10$ and $k^{(1)} = 1$) at $t = 0.4$.

smaller than that in the high-permeability layer; this dimension is 0.15 and 0.20, respectively. Thus, although an increase in the permeability leads to an increase in the rate of displacement and oil recovery, an increase in the degree of nonuniformity results in a larger amount of the micellar solution flowing into the high-permeability layer and, hence, the effectiveness of displacement from the bottom layer reduces. In this case, an increase in the volume of the bank moving in the high-permeability layer virtually does not lead to an increase in the oil recovery from this layer. At the same time, the volume of the part of the bank in the low-permeability layer decreases because of the cross-flow to the other layer, and, hence, the effectiveness of displacement from the layer with $k^{(1)} = 1$ decreases.

An analysis of the current oil extraction coefficient — the main process parameter — for various volumes of the micellar bank with $k^{(2)} = 8$ shows that, although for the volumes considered, the oil bank reaches the exit from the layer almost simultaneously, the amount of oil confined hydrodynamically in the porous medium is different: it is larger the smaller the bank size. In the case of nonuniform reservoirs, the oil bank reaches the productive well more rapidly because of the presence of a high-permeability layer, but, in this case, the oil recovery is significantly lower because of the displacement nonuniformity.

Figure 8 shows isobars for a nonuniform layered reservoir ($k^{(2)} = 10$) for a volume of the injected micellar fluid bank $t_{\text{m}} = 0.1$ at the time $t = 0.4$. In almost the entire filtration region, the field of velocities whose direction should be normal to the isobars is parallel to the x axis, i.e., the motion is nearly one-dimensional. The pressure at the entrance into the bottom, less permeable layer is higher than that at the entrance to the top layer. The location of the isobars near the injection line indicates that part of the fluid injected into the low-permeability layer flows into the top high-permeability layer. We also note that, in comparison to the square filtration region (version of oil displacement by water) the dimension of the cross-flow region in this case is significantly smaller and the motion in the layers is closer to one-dimensional motion.

2. Results of Numerical Simulation of Micellar–Polymer Extraction of Oil from a Nonuniform Layered Reservoir for a Specified Pressure Difference. The micellar–polymer flooding of a nonuniform layered reservoir for a specified pressure difference between the entrance and exit from the porous medium was studied. The model for the reservoir and the characteristics of the micellar–polymer flooding are the same as

in [3–5]. The boundary condition on the pressure on the segments AC and DF (see Fig. 1) is specified in the form $p(d'\Omega, t) = p(t)$. In this problem, the independent variable on which the oil recovery coefficient η depends is taken to be the dimensionless volume of the injected fluid normalized by the reservoir pore volume τ.

For the micellar–polymer flooding of nonuniform layered reservoirs with a specified pressure difference, the effect of two factors on the effectiveness of the process was studied: the degree of macrononuniformity of the oil reservoir thickness and the volume of the micellar fluid bank injected into the layer. The following micellar-flooding regime was analyzed numerically. The reservoir had a rectangular section ($l_x = 1$ and $h = 0.01$). The two layers constituting the reservoir (see Fig. 1) had identical thickness and porosity. The pore space of this layer was initially saturated with water and oil ($s_{10}^0 = 0.26$), whose viscosities were $\mu_{\rm w} = 1$ and $\mu_{\rm oil} = 6$, respectively. The curves of the relative phase permeabilities for the joint filtration of water and oil are the same as in [3–5].

The displacing fluids injected into the layer had the following characteristics: the viscosity of the micellar solution of the initial composition was 9.7, and the viscosity of the polymer solution used as the spacer fluid was 14 (with the drag taken into account). The volume of the micellar fluid bank was varied, and the volume of the second injected polymer solution bank was constant: $V_{\rm p} = 0.6V_{\rm pore}$. The relative phase permeabilities of the hydrocarbon phase containing SASs and the water phase were calculated according to [3–5] (as previously, a micellar solution was used that dissolved reservoir oil but not water).

For the flooding versions considered, the pressure difference between the reservoir entrance ($\hat{p} = 5$) and exit ($\tilde{p} = 1$) was specified as the boundary condition. The calculations were performed on a 20×10 finite-difference grid ($\Delta x = 0.05$ and $\Delta y = 0.001$) for $\Delta t = 0.003$, the iteration step was $\delta = 0.065$, and the admissible error in the condition of convergence of the iterative process in the determination of the pressure was $\varepsilon = 1/40$.

The following integral characteristics were analyzed: the flooding effectiveness of the nonuniform layered reservoir and the total oil recovery coefficient η versus the dimensionless volume of the injected fluid τ normalized by the reservoir pore volume $V_{\rm pore}^0$ for various values of the absolute permeability of the top layer ($k^{(1)} = 1$) and the volume of the injected micellar fluid bank $\tau_{\rm m}$ normalized by the reservoir pore volume. Curves of $\eta(\tau)$ characterize the step-by-step oil displacement from the layers. The reservoir oil and water with watering corresponding to the initial oil saturation are driven first. Then, the water-oil bank formed in the top high-permeability layer approaches the exit. After that, oil from the bank in the bottom layer begins to flow out. We note that increasing the macrononuniformity improves the displacement in the high-permeability layer (earlier approach of the bank to the exit, and the higher oil saturation in it). However, in this case, the displacement virtually does not cover the bottom layer. As a result, the final oil recovery decreases considerably. This, for reservoirs with $k^{(2)} = 2$ and $k^{(2)} = 10$ for $\tau_{\rm m} = 0.1V_{\rm pore}$ in the case of injection of two reservoir pore volumes ($\tau = 2V_{\rm pore}$), it was 99 and 71% respectively, which confirms the qualitative conclusion drawn from experimental results [7].

The use of a simplified "rigid stream tube method" for calculating micellar–polymer flooding was studied in [8].

Conclusions. The dynamics and effectiveness of oil displacement from a layered reservoir of nonuniform thickness consisting of two hydrodynamically connected layers with different absolute permeability were studied.

For the flooding regime at a specified injection rate, the layer-by-layer motion of the displacing water and the current oil recovery were studied for various absolute permeabilities of one of the layers and various shapes of the filtration region. It was established that the degree of nonuniformity depends significantly on the reservoir geometry. Thus, for a filtration region of square shape, the time of water-free oil production $t_{\rm influx}$ (at the beginning of the process, water was in the connected state in the porous medium) depended little on the value of $k^{(2)}$ in the examined range of its values ($k^{(2)} = 1$–10), and for a filtration region of rectangular shape (the ratio of the reservoir thickness h to length was 0.06) value $t_{\rm influx}$, it varied from 0.6 to 0.32.

In the case of micellar–polymer flooding, the filtration flow and oil recovery were studied for various permeabilities of one layer $k^{(2)}$ (from 1 to 10) and various volumes of the fluid bank $V_{\rm m}$ (from $0.1V_{\rm pore}$ to $0.02V_{\rm pore}$). From the analysis of the isobars, it follows that for the specified flow rate, the cross-flow between the layers occurs in the vicinity of the injection line. The break of the bank and the displacement nonuniformity in the layers are due to the fact that an increase in the nonuniformity leads to an increase in the volume of the injected bank moving in the high-permeability layer. A similar study performed at a specified pressure also showed that the nonuniformity had a negative effect on oil recovery.

We thank R. I. Nigmatulin for useful discussions.

REFERENCES

1. M. L. Surguchev, *Secondary and Tertiary Methods of Enhancing Reservoir Oil Recovery* [in Russian], Nedra, Moscow (1985).
2. K. Aziz and A. Settari, *Petroleum Reservoir Simulation*, Applied Science Publsihers, New York–London (1979).
3. R. I. Nigmatulin, K. M. Fedorov, and N. S. Khabeev, "Mathematical simulation of micellar–polymer displacement of oil from flooded reservoirs," *Izv. Akad. Nauk. SSSR, Mekh. Zhidk. Gaza*, No. 6, 84–93 (1982).
4. R. I. Nigmatulin, K. M. Fedorov, and N. S. Khabeev, "Numerical study of micellar–polymer displacement of oil from nonuniform layered reservoirs," *Izv. Akad. Nauk. SSSR, Mekh. Zhidk. Gaza*, No 2, 87–93 (1984).
5. N. A. Inogamov and N. S. Khabeev, "Simulation of micellar–polymer flooding in a system of wells," *Izv. Ross. Akad. Nauk, Mekh. Zhidk. Gaza*, No. 6, 124–132 (2004).
6. V. M. Entov and A. M. Polishchuk, "Role of adsorption processes during motion of polymer solutions in porous media," *Izv. Akad. Nauk. SSSR, Mekh. Zhidk. Gaza*, No. 3, 68–75 (1975).
7. V. A. Shirokov, "Experimental study of the motion of banks of chemical reactant used in porous media to enhance oil recovery," Doct. Dissertation in Tech. Sci. (1979).
8. N. A. Inogamov and N. S. Khabeev, "Using the rigid stream tube method to calculate micellar–polymer flooding in a staggered system of wells," *Inzh.-Fiz. Zh.*, **80**, No. 1. 15–21 (2007).